Published in : Current Protocols in Microbiology *(2024), vol. 4, 1043*
DOI: https://doi.org/10.1002/cpz1.1043
Status : Postprint (Author's version)

COMPARISON OF THREE WIDELY EMPLOYED EXTRACTION METHODS FOR METABOLOMIC ANALYSIS OF *TRYPANOSOMA BRUCEI*

Fanta Fall,[1,5] Lieven Desmet,[2] Lucia Mamede,[3] Laura Schioppa,[1] Pascal de Tullio,[4] Michel Frédérich,[3] Bernadette Govaerts,[2] and Joëlle Quetin-Leclercq[1]

[1]*Pharmacognosy Research Group, Louvain Drug Research Institute (LDRI), Université Catholique de Louvain (UCLouvain), Brussels, Belgium*

[2]*Institute of Statistics, Biostatistics and Actuarial Sciences (ISBA/LIDAM), UCLouvain, Louvain-la-Neuve, Belgium*

[3]*Laboratory of Pharmacognosy, Center for Interdisciplinary Research on Medicines (CIRM), University of Liège, Belgium*

[4]*Metabolomics group, Center for Interdisciplinary Research on Medicines (CIRM), University of Liège, Belgium*

[5]*Corresponding author: fanta.fall@uclouvain.be*

Published in the Microbiology section

KEYWORDS: extraction • mass spectrometry • metabolomics • *Trypanosoma brucei*

ABSTRACT

Trypanosoma brucei (Tb) is the causative agent of human African trypanosomiasis (HAT), also known as sleeping sickness, which can be fatal if left untreated. An understanding of the parasite's cellular metabolism is vital for the discovery of new antitrypanosomal drugs and for disease eradication. Metabolomics can be used to analyze numerous metabolic pathways described as essential to *Tb. brucei* but has some limitations linked to the metabolites' physicochemical properties and the extraction process. To develop an optimized method for extracting and analyzing *Tb. brucei* metabolites, we tested the three most commonly used extraction methods, analyzed the extracts by hydrophilic interaction liquid chromatography high-resolution mass spectrometry (HILIC LC-HRMS), and further evaluated the results using quantitative criteria including the number, intensity, reproducibility, and variability of features, as well as qualitative criteria such as the specific coverage of relevant metabolites. Here, we present the resulting protocols for untargeted metabolomic analysis of *Tb. brucei* using (HILIC LC-HRMS).

Basic Protocol 1: Culture of *Trypanosoma brucei brucei* parasites

Basic Protocol 2: Preparation of samples for metabolomic analysis of *Trypanosoma brucei brucei*

Basic Protocol 3: LC-HRMS-based metabolomic data analysis of *Trypanosoma brucei brucei*

INTRODUCTION

Trypanosoma brucei (*Tb*) is the causative agent of sleeping sickness, a disease affecting sub-Saharan Africa. This species is divided into three subspecies, two affecting humans (*Trypanosoma brucei gambiense* and *Trypanosoma brucei rhodesiense)* and one affecting animals (*Trypanosoma brucei brucei*) (Brun et al., 2010; Hannaert, 2011). Two forms of the parasite have been described in the literature: the bloodstream form (BSF) and the procyclic form (in the vector) (Matthews, 2005). A better knowledge of the parasite's cellular metabolism would allow better management of current issues with toxicological and resistance (WHO, n.d.) and a deeper understanding of the important metabolic pathways that could lead to the discovery of relevant therapeutic targets.

Metabolomics is the latest of the 'omics sciences that developed around the 1990s (Johnson et al., 2016); it enables the analysis of mixtures of molecules with molecular weights <1400 Da (Vincent & Barrett, 2015). Liquid or gas chromatography coupled with high-resolution mass spectrometry (GC-HRMS and LC-HRMS) or nuclear magnetic resonance (NMR) are the major techniques used for metabolomic analyses. LC-HRMS generates qualitative and/or quantitative data about an organism's metabolome, which comprises a set of molecules with different physicochemical properties. Because of the large size and chemical variety of the metabolome, no single analysis or extraction technique is sufficient to cover the entire metabolite profile. The standardization of experimental protocols in metabolomics is an area of major debate owing to the multiple parameters that can influence metabolite extraction and detection (Bi et al., 2013; Martin et al., 2014). Depending on the type of metabolomics analysis (targeted or untargeted), different protocols and extraction solvents (including mixtures of solvents) can be used, and these choices directly influence the detection quality of intracellular metabolites. There are multiple methods available in the literature, and it is important to take into consideration the purpose of the analysis when making this choice (Fall et al., 2022). Notably, the choice of the extraction solvent or mixture is essential to assess reproducible and sensitive analysis and improve the number of metabolites detected from different chemical classes, ensuring diversity (Pinu et al., 2017).

Published in : Current Protocols in Microbiology *(2024), vol. 4, 1043*
DOI: https://doi.org/10.1002/cpz1.1043
Status : Postprint (Author's version)

Depending on its form (BSF or procyclic) and the environment in which it is found, *Tb. brucei* obtains its energy from glucose (carbohydrate metabolism) or amino acids such as proline and arginine (amino acid metabolism) (Bakker et al., 1999; Villafraz et al., 2021). Some amino acids are used in the biosynthesis of fatty acids that are essential for the parasite (Smith et al., 2017). As each class of compounds has different chemical properties (in terms of lipophilicity, stability, molecular weight, etc.), various extraction methods have been described for metabolomics analyses of *Tb. brucei* samples. After cell culture, parasites are usually soaked in liquid nitrogen or in a dry ice/ethanol bath to stop the metabolism and minimize any further metabolite turnover in a process named quenching. Before an extraction solvent is applied, parasites are isolated and washed to remove the medium.

Many different types of parasites can also induce pathologies and are thus interesting to explore through metabolomics. Several studies have sought to achieve this for parasites such as *Plasmodium*, *Leishmania*, and *Toxoplasma*, among others, and follow the same general workflow as just described for the *Trypanosoma*—cell culture, quenching, washing and extraction (Amiar et al., 2020; Rey-Stolle et al., 2022; Song et al., 2023; Vincent & Barrett, 2015). These techniques have been reviewed elsewhere, but it is interesting to note the similarities in extraction methodologies across studies. Not only are the work- flow stages relatively uniform, but so are the extraction methods and solvents, including the data acquisition methods (Vincent & Barrett, 2015). The methods explored in this protocol have generally been used to study other pathogens as well, with differences pertaining to handling the culture, sampling, and data interpretation (Fall et al., 2022; Kafsack & Llinas, 2010; Mamede et al., 2022; Vincent & Barrett, 2015). Metabolomics as an approach is useful regardless of the parasite being studied, and needs only to be adapted to their lifeform, stage, number, and culture conditions. Similarly, different methods might prove to be optimal with different parasites depending on these conditions and on the metabolites/pathways that are the objective of the study or specific to the parasite analyzed.

Basic Protocol 1 describes parasite culture procedures designed for optimal survival and growth.

Basic Protocol 2 presents the three extraction methods that we compared in our recent study, which we chose on the basis of their use in untargeted trypanosome metabolomic assays reported in the literature (Fall et al., 2022). Method 1 (M1) involves a mixture of 1:3:1 (v/v/v)

chloroform/methanol/water that has been used in several *Tb. brucei* metabolomic studies identifying metabolic pathways (Creek et al., 2015; Johnston et al., 2019; Vincent & Barrett, 2015) such as the Krebs cycle, amino acid biosynthetic pathways, glycolytic pathway, and nucleoside and nucleotide biosynthetic pathways (Creek et al., 2015; Johnston et al., 2019; Vincent & Barrett, 2015). Method 2 (M2) features a mixture of 4:4:2 (v/v/v) acetonitrile/methanol/water that has been used to analyze glycerol metabolism and the metabolisms of other molecules such as alanine, fumarate, phosphoenolpyruvate, 6-phosphogluconate, and succinate (Pineda et al., 2018). Method 3 (M3) is derived from the Bligh and Dyer extraction technique using 1:2:1 (v/v/v) methanol/chloroform/water and applied to the lipid metabolome of *Tb. brucei*, specifically glycerophospholipids (Richmond et al., 2010).

Basic Protocol 3 details conditions for the analysis and acquisition of metabolomic data. We describe the filters and treatments to be applied to the LC-HRMS spectra to obtain high-quality metabolomic data. Hydrophilic interaction liquid chromatography (HILIC) coupled with high-resolution mass spectrometry (HRMS) has been identified as a good system to analyze the intracellular metabolome of *Tb. brucei*. HILIC-LC-HRMS mainly allows the analysis of polar metabolites in the *Tb. brucei* metabolome (Kamleh et al., 2008; t'Kindt et al., 2010). In our study we compared, for the first time (to our knowledge), the three methods mentioned above to identify the best option for extracting the maximum amount of intracellular *Tb. brucei* metabolites with the highest level of reproducibility and sensitivity (Fall et al., 2022). The influence of protocol and solvent on detection accuracy, intensity, reproducibility, and identified metabolite classes is determined by HILIC-LC-HRMS. Our analysis indicated that method 2, involving an extraction with 4:4:2 (v/v/v) acetonitrile/methanol/water and a 20-min incubation, allowed the most complete untargeted analysis of the trypanosome metabolome, based on greater robustness and higher numbers of unique features detected and pathways annotated. It is worthwhile to mention that the analytical conditions and type of study (untargeted or targeted) might lead to a different outcome. In the latter case, different extraction methodologies might be more appropriate, depending on what part of the trypanosome metabolome the study is meant to focus on (Fall et al., 2022).

CULTURE OF *Trypanosoma brucei brucei* PARASITE CULTURE

BASIC PROTOCOL 1

Parasites used are *Tb. brucei* BSF (strain stock 427; Vertommen et al., 2008), as previously described

Published in : Current Protocols in Microbiology *(2024), vol. 4, 1043*
DOI: https://doi.org/10.1002/cpz1.1043
Status : Postprint (Author's version)

(Hirumi & Hirumi, 1994). Briefly, parasites are maintained under sterile conditions at densities between 1 x 106/ml and 1.5 x 10^6/ml and diluted 100- or 1000- fold every 2 or 3 days, respectively. The number of living trypanosomes is counted using a Bürker chamber. For the metabolomic analysis, four cultures of *Tb. brucei* are prepared (flasks F1, F2, F3, and F4). From each flask, two samples were collected, of which two each were extracted according to methods M1, M2, or M3.

Figure 1 *Experimental design of parasite cultures.*

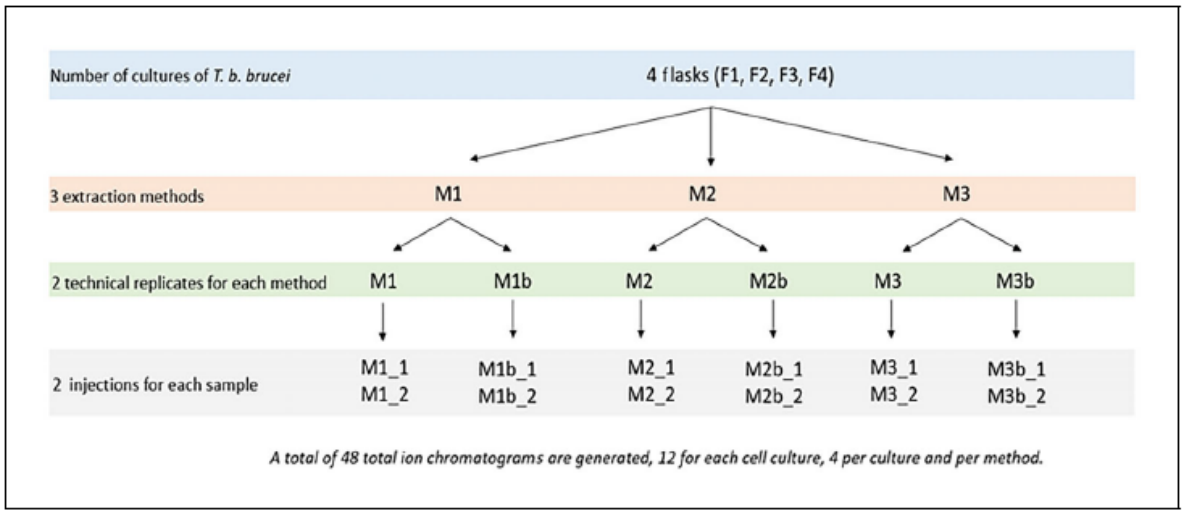

For simplification purposes, the nomenclature for each sample reflected the origination flask, the extraction method, and the duplicate standing: e.g., F1M1 is a sample collected from F1 and extracted with M1, and F1M1b is prepared using the same conditions but is the second replicate (Fig. 1).

MATERIALS

Frozen culture flask of *Tb. brucei* strain 427

HMI9 medium (see recipe)

Fetal bovine serum (FBS), -20°C

L-Cysteine

24-well plate, sterile

50- and 10-ml transfer pipets, sterile

20-, 200-, and 1000-µl pipets, sterile

37°C, 5% CO_2 incubator

Inverted microscope with phase-contrast optics

25. and 175-cm^3 (T25 and T175) culture flasks

Water bath

Bürker chamber

50-ml conical polystyrene tubes (Falcon)

DEFROSTING AND CULTURE OF PARASITE STRAINS

1. Before removing the culture flask from -80°C freezer or liquid nitrogen, prepare supplemented HMI-9 medium supplemented with FBS and L-cysteine (see recipe).
2. Add 1 ml of this medium to the 6 wells of the first two rows of a 24-well plate.
3. Remove the culture flask from cryopreservation (-80°C freezer or liquid nitrogen).
4. Let the culture flask defrost completely at room temperature.
5. Once the last ice has disappeared, collect the parasites as quickly as possible, pipetting up and down several times to homogenize the culture. Then transfer to the 24- well plate as follows:
   a. Transfer 100 pl of the culture flask contents into each of the 6 wells in the first row of the 24-well plate.
   b. Transfer 100 pl from each well of the first row and into the corresponding wells of the second row (performing a direct a 10 x dilution to decrease the concentration of the glycerol used for cryopreservation).
6. Incubate 2 days in a 37°C, 5% CO_2 incubator.
7. After the 2 days, remove 100 pl from one of the two central wells of the second row and transfer to 25-cm^3 flask containing 10 ml medium.

MAINTENANCE OF PARASITE CULTURE AND PREPARATION OF THE CULTURE FLASK FOR EXTRACTION

8. Every second day, check the culture by microscopic observation and then dilute to 1/10 concentration: Take 1 ml of the ongoing culture and transfer into a new 25-cm^3 flask containing 9 ml HMI9 medium prewarmed to 37°C in a water bath.
9. Every fifth day, perform a 1/100 dilution by taking 100 pl of the culture and transferring it into a new 25-cm^3 flask containing 10 ml HMI9 medium prewarmed to 37°C in a water bath.
10. To prepare for the metabolomic assay, count the number of parasites using a Bürker chamber with a microscope and calculate the volume needed to collect 100,000 trypanosomes.
11. To prepare four culture flasks (175 cm^3 each) containing F1, F2, F3, and F4, place 100,000 trypanosomes in 100 ml of supplemented HIM9 culture medium prewarmed to 37°C.
12. Incubate 3 days at 37°C, 5% CO_2.
13. After the 3 days of incubation, count the number of trypanosomes per milliliter of medium. In

Published in : Current Protocols in Microbiology *(2024), vol. 4, 1043*
DOI: https://doi.org/10.1002/cpz1.1043
Status : Postprint (Author's version)

our experiment, we found the following: F1 =15.6 x 10^5 trypanosomes/ml, F2 = 16.5 x 10^5 trypanosomes/ml, F3 = 22.5 x 10^5 trypanosomes/ml, and F4 = 14.8 x 10^5 trypanosomes/ml.

14. From each flask, prepare six samples by pipetting into 50-ml Falcon tubes, using sterile transfer pipets, the appropriate volume needed to achieve 2.5 x 10^7 trypanosomes/sample (in our experiment, for examples, the six for F1 were F1M1 + F1M1b, F1M2 + F1M2b, and F1M3 and F1M3b). Do the same for F2, F3, and F4, for a total of 24 samples (Fig. 1).

The samples are now ready for quenching and extraction as detailed in Basic Protocol 2.

SAMPLE PREPARATION FOR METABOLOMIC ANALYSIS OF *Trypanosoma brucei brucei*

BASIC PROTOCOL 2

After the culture step, a quenching method was applied to all samples of the four culture flasks (F1, F2, F3, and F4) to stop parasite metabolism. Three extraction methods (M1, M2, and M3) were applied to all the flasks. The samples were prepared in replicates and injected in replicates in the LC-HRMS system (Fig. 1). In this section, we describe the preparation stages for the three extraction methods. All samples are kept in cold conditions (ice bath) whenever otherwise stated.

MATERIALS

Acetonitrile, HPLC grade (VWR)

Methanol, HPLC grade (VWR)

Water, HPLC grade and LC-HRMS grade (VWR)

Chloroform, HPLC grade (VWR)

Dry ice

Ethanol

Aliquots of 2.5 x 10^7 parasites/sample (Basic Protocol 1)

Phosphate-buffered saline (PBS)

0.1% formic acid (VWR)

2-ml microcentrifuge tubes

20-, 200-, and 1000-µl calibrated micropipets

Ice bucket

Refrigerated centrifuge, 4°C

Automatic agitator

Glass vials with micro-inserts for LC-HRMS analysis

Vortex

Speedvac (CentriVap, General Equipment-BRS)

Sonication bath

Nitrogen gas (flow)

PREPARE THE EXTRACTION SOLVENTS

1. For M1, prepare 1 ml of 1:3:1 (v/v/v) chloroform/water/methanol extraction mixture (0.1 ml per sample, 8 in total to be extracted by M1) and store at -20°C until use.
2. For M2, prepare 15 ml of 4:4:2 (v/v/v) acetonitrile/methanol/water extraction mixture (1.5 ml per sample, 8 in total to be extracted by M2) and store at -20°C until use.
3. For M3, prepare the two extraction solvents: 5 ml of 1:1 (v/v) water/methanol (0.5 ml per sample, 8 in total to be extracted by M3) and 5 ml chloroform (0.5 ml per sample, 8 in total to be extracted by M3). Store at -20°C until use.

   The extraction solvents should be prepared a few hours before sample extraction, to allow time for them to cool, assuring a low temperature that won't facilitate metabolite turnover, while avoiding contamination or other issues that could arise during longer- term storage. It is advisable to always prepare a bit more than calculated (e.g., the 1 ml instead of 0.8 ml calculated for M1).

QUENCHING AND WASH

4. Quench samples by rapid (20 s) cooling in a dry ice/ethanol bath.
5. Centrifuge samples 20 min at 1250 rcf, 4°C, to separate the parasites from the culture medium.
6. Discard the supernatant and resuspend the pellet with 2 mlof 1 x PBS.
7. Transfer samples to 2-ml microcentrifuge tubes.
8. Wash the samples twice by centrifuging for 10 min at 1250 rcf, 4°C, and removing the supernatant.
9. Separate the samples by the planned extraction method and then extract them by following Extraction Method 1 (steps 10a-13a) for M1, Extraction Method 2 (steps 10b-15b) for M2, and Extraction Method 3 (steps 10c-15c) for M3.

EXTRACTION METHOD 1 (M1)

10a. Starting with the "M1" microcentrifuge tubes that you previously prepared and labeled—F1M1,

Published in : Current Protocols in Microbiology *(2024), vol. 4, 1043*
DOI: https://doi.org/10.1002/cpz1.1043
Status : Postprint (Author's version)

F1M1b, F2M1, F2M1b, F3M1, F3M1b, F4M1, and F4M1b—add 100 pl of 1:3:1 (v/v/v) chloroform/water/methanol extraction mixture at 0°C (ice bath) (from step 1) to each sample.

11a. Agitate vigorously for 1 hr using an automatic agitator.

12a. Centrifuge 10 min at 9000 rcf, 4°C.

13a. Transfer supernatant into glass vials with micro-inserts and cap immediately for LC-HRMS analysis.

EXTRACTION METHOD 2 (M2)

10b. Starting with the "M2" microcentrifuge tubes that you previously prepared and labeled—F1M2, F1M2b, F2M2, F2M2b, F3M2, F3M2b, F4M2, F4M2b—add 1.5 ml of 4:4:2 (v/v/v) acetonitrile/methanol/water extraction mixture at 0°C (ice bath) to each cell pellet.

11b. Vortex and incubate samples for 20 min at -20°C.

12b. Dry supernatant using the Speedvac centrifuge concentrator.

13b. Resuspend with 150 pl ultrapure water (LC-HRMS quality).

14b. Centrifuge tubes 2 min at 4000 rcf, 4°C.

15b. Immediately transfer supernatant into glass vials with micro-inserts and cap for LC-HRMS analysis.

EXTRACTION METHOD 3 (M3)

10c. Starting with the "M3" microcentrifuge tubes that you previously prepared and labeled—F1M3, F1M3b, F2M3, F2M3b, F3M3, F3M3b, F4M3, and F4M3b—add 500 µl of 1:1 (v/v) water/methanol and 500 µl chloroform at 0°C (ice bath) to each cell pellet.

11c. Sonicate the mixture in the sonication bath for 10 min and then stir samples with the automatic agitator for 10 min.

12c. Centrifuge tubes 5 min at 4000 rcf, 4°C.

13c. Collect the upper phase in microcentrifuge tubes and dry under nitrogen flow.

14c. Reconstitute samples with 75 µl of 20:80 (v/v) formate/acetonitrile.

15c. Immediately transfer supernatant into glass vials with micro-inserts and cap for LC-HRMS analysis.

LC-HRMS-BASED METABOLOMIC DATA ANALYSIS OF *Trypanosoma brucei brucei*

BASIC PROTOCOL 3

For a better understanding of this protocol, a diagram is provided showing the organization of the different extractions and injections in the LC-HRMS procedure (Fig. 1).

MATERIALS

Solvent A: 10 mM ammonium formate (see recipe), pH 3.8

Solvent B: Acetonitrile

HILIC column: Phenomenex Luna 3 mm x 150 mm, 200 A HILIC (Louvain, Belgium)

LC-HRMS system consisting of a Thermo Accela pump, autosampler, photodiode array detector, and Thermo Scientific LTQ orbitrap XL mass spectrometer with an ESI interface

Thermo Scientific™ Xcalibur™ software (associated with the LC-HRMS system)

ProteoWizard (*https:// proteowizard.sourceforge.io/*)

Worklow4Metabolomics 3.3 (W4M) (*https:// workflow4metabolomics.org/*)

Metaboanalyst (*https:// www.metaboanalyst.ca/*)

R (base packages, limpca package, version 4.3.1)

LC-HRMS analysis

1. Perform LC gradient elution on HILIC column set at 40°C with a flow rate of 0.3 ml/min: start with 5% solvent A for 3 min, increase to reach 95% solvent A at 25 min, maintain for 5 more min, decrease back down to 5% solvent A, and finally equilibrate for 10 min for a total run time of 40 min.
2. Analyze samples by mass spectrometry using an ESI mass spectrometer with the ESI interface operating in positive-ion mode, using the following settings: capillary voltage, 2.8 kV; sheath gas flow rate, 60; auxiliary gas flow rate, 30; temperature capillary, 325°C; S-lens RF level, 155).
3. Inject 10 pl of each sample following a randomized plan.
4. Use a full scan mode (60-900 *m/z*) with a mass resolution of 60,000.
5. Perform data acquisition and processing with Xcalibur™ software.

Published in : Current Protocols in Microbiology *(2024), vol. 4, 1043*
DOI: https://doi.org/10.1002/cpz1.1043
Status : Postprint (Author's version)

METABOLOMIC DATA ANALYSIS

6. Pre-processing and filtering: Convert the raw LC-HRMS data profiles in mzXML format with ProteoWizard (Adusumilli & Mallick, 2017).
7. Process mzXML format files using the XCMS package (Smith et al., 2006) into Worklow4Metabolomics 3.3 (W4M) (Giacomoni et al., 2015)
8. Filter out (Blank-over-Bio-ratio filter) features detected in blank samples with intensity in blanks of >0.5 times the mean intensity observed in biological samples
9. Perform metabolite identification with Metaboanalyst (Chong et al., 2018) using the "Functional analysis" module and the "Peak intensity table" tab with the *m/z* list. In our experiments, we selected the following parameters:
    a. Ion mode: positive mode
    b. Mass tolerance (ppm): 10 ppm
    c. Retention time: none
    d. Data source: generic
    e. Data format: samples in columns
    f. Filtering: none
    g. Data scaling: pareto scaling
    h. Algorithms: Mummichog visualized with Scatter Plot
    i. Pathway library: *Trypanosoma brucei brucei* [KEGG]
10. Cross-reference the identification against the Kyoto Encyclopedia of Genes and Genomes (KEGG) database (*https:// www.kegg.jp/;* Kanehisa & Goto, 2000) with *Tb. brucei* selected.
11. Perform appropriate statistical analyses and data plots with the open-source R software (R, n.d.): namely, PCA, ASCA, heatmap, and a summary with the aggregated results.
12. To determine the best extraction method, we analyze four criteria: the number of features detected, their reproducibility (reproducible ion detection in replicates), the signal intensity, and the variability of the measured intensities.
13. Log-transform (i.e., calculate log(x+1)) the intensities (x) before analyzing of the four criteria.

REAGENTS AND SOLUTIONS

Ammonium formiate, pH 3.8, 10 mM

Weigh out ammonium formiate to a final concentration of 10 mM (e.g., 630 mg in 1 liter of MilliQ

water). Adjust pH to 3.8 with formic acid, testing with a pH meter. Filter using a Nylaflo 0.45-µM, 47-mm nylon filter (cat. no. 46000351). Store up to 1 week at 4°C.

HMI9 medium stock

Weigh out the following components to obtain the desired concentrations:

1 mM hypoxanthine (Acros 122010250)

36 mM $NaHCO_3$

1 mM sodium pyruvate (Merck 1.06619.0050)

0.16 mM thymidine (Acros 226740050)

0.04 mM bathocuproine disulfonate (Acros 164060010)

10% (v/v) heat-inactivated fetal bovine serum (FBS)

20 mM 2-mercaptoethanol

150 mM L-cysteine

Add 1/10 of the final planned volume of MilliQ water and shake for 2 hr to dissolve the compounds. Check that all of the compounds are dissolved and then dilute to final volume. Adjust to pH 7.2 with 37% concentrated hydrochloric acid using a pH meter.

Place a 0.2- pm-pore-size filter (Sartolab P20plus from Sartorius, 0.2 pm PES, filtration area 20 cm^2 and filtration volume up to 10 liters, with hose inlet; Sartorius part number 18091-D) on the peristaltic pump and pass 200 ml MilliQ water through it. Filter the prepared medium through the Sartolab P20Plus filter. Rinse the entire system with 200 ml MilliQ water and then discard the filter.

Store the filtered medium for up to 6 months at 4°C.

HMI9 medium, supplemented

Heat-inactivate FBS for 35 min at 56°C, and prepare 5 ml filtered cysteine mixture as follows:

Place 182 mg L-cysteine in a 25-cm^3 flask

Add 10 ml MilliQ water and 14 µl of 2-mercaptoethanol

Dissolve by vortexing

Filter with a 0.22-pm-pore size sterile filter

Just before use, prepare supplemented HMI9 medium by add 50 ml FBS and 5 ml of the filtered L-cysteine mixture to 450 ml of HMI9 medium stock (see recipe).

Published in : Current Protocols in Microbiology *(2024), vol. 4, 1043*
DOI: https://doi.org/10.1002/cpz1.1043
Status : Postprint (Author's version)

COMMENTARY

BACKGROUND INFORMATION

The intracellular metabolome of *Tb. brucei* is highly diverse, making it impossible to analyze in its entirety using a single universal technique. To date, several methodologies have been used to overcome this bio- logical complexity (Creek et al., 2015; Fall et al., 2022; Johnston et al., 2019; Pineda et al., 2018; Zoltner et al., 2020). The advantage of untargeted metabolomics is the ability to find specific metabolic signatures within an organism. The extraction protocol must be minimally invasive and be carried out so as to minimize unwanted variation. Procedures for extracting metabolites from the cellular environment often involve the use of organic solvents, with or without water or other chlorinated solvents, at different temperatures and pH (Madji Hounoum et al., 2016). Various studies have shown that different solvent- based extraction methods can yield significantly different metabolic profiles, which has a significant impact on the biological interpretation of metabolomic data. We have chosen to compare several reported methods that have been used to analyze *Tb. brucei* over the years, and sought to choose the most re- producible method based on our comparative criteria after HILIC HPLC-HRMS untargeted analysis. It is, however, worth mentioning that each method, based on the nature of the solvent and the form and time of incubation, among other potential factors, may vary in the range of the metabolome extracted. For example, the Bligh and Dyer method (method 3 in this assessment) has long been considered the standard method for extracting lipid metabolites. It produces two phases, polar and apolar, that are supposed to be analyzed with a normal-phase column and a reverse-phase column, respectively. In this work, we only subjected the aqueous phase to analysis on one (HILIC) column, so some apolar compounds may have been lost in the organic phase in our application of method 3. On the other hand, methods 1 and 2 may not extract apolar compounds as extensively as method 3 and thus should not be used when specifically searching for this part of the trypanosome metabolome. In our assessment, our purpose was to choose a method that provides the largest and most re- producible set of features in order to achieve an untargeted metabolomics method that is as robust as possible. If the purpose of the experimental work is to investigate a set of particular metabolites, the extraction protocol should be adapted accordingly.

Table 1 *Troubleshooting Guide for Untargeted Metabolomic Analysis with Tb. brucei*

Problem	Possible cause	Solution
Insufficient enough parasites to begin metabolomics assay	Age of the culture	Growth rate depends on the age of culture (time post thawing). If culture age is >6 months, consider defrosting a new culture.
	Problems with culture vessels or medium	Prepare multiple flasks and/or new culture medium.
	Incubator settings	Verify that the incubator is set to 37°C, 5% CO_2.
Failure to include the entire M3 extract	Extract has separated into a polar and a nonpolar phase	Before collecting the upper phase to be dried, let the samples rest to achieve full separation. Use reverse-phase liquid chromatography (RP-LC) to analyze the lipophilic phase.

CRITICAL PARAMETERS

In untargeted metabolomics, it is crucial to use techniques that minimize additional variability beyond that associated with anything other than the factors under study. Although diminishing such variability should be the goal, targeted analysis is less susceptible to variability than untargeted analysis. In a targeted design, the metabolites to be found are known and the workflow is usually optimized to find them. In untargeted metabolomics, the purpose is to find as many metabolites as possible to obtain the maximum biological information, and as such, any confounding factors need to be reduced. Ideally, the same experimenter should perform all of the analysis to avoid extra variation. In parasite cultures, not all parasites are at the same growth stage, which can affect the results, as the metabolic profile of *Tb. brucei* may vary among parasites at different life stages, affecting the outcome of metabolomic analysis. To ensure accurate results, it is necessary to use multiple cell culture replicates to verify that differences observed between extraction methods are real, regardless of the *Tb. brucei* culture. It is also important to accurately count the number of parasites before extraction and standardize the number of parasites used for the analysis.

TROUBLESHOOTING

A few complications may arise during the execution of this protocol. A condensed troubleshooting guide is provided in Table 1.

STATISTICAL ANALYSIS

Different tools were used to compare and select the best method to perform an untargeted metabolomic analysis of the *Tb. brucei* metabolome. In a first instance, several visualization tools

Published in : Current Protocols in Microbiology *(2024), vol. 4, 1043*
DOI: https://doi.org/10.1002/cpz1.1043
Status : Postprint (Author's version)

were used to explore the data: principal component analysis (PCA), heatmaps, and Venn diagrams. PCA is a common data reduction and visualization technique used in metabolomics to identify patterns in high-dimensional data. By comparing the first few principal components between methods, it is possible to get a sense of how similar or different the methods are in their ability to capture the underlying structure in the data and visualize inter-and intra-group variability. When the design is multifactorial, ASCA+ can advantageously supplement PCA to help visualize the difference between levels of less important factors and the intra-group variability after the deletion of the factor effects (Thiel et al., 2017). It also makes it possible to test the global significance of factor effects and quantify their relative importance (Thiel et al., 2023). Heatmaps are a type of data visualization tool that display the values of two or more variables in a color-coded grid format. The data are organized into a matrix, with the rows and columns representing the variables of interest. Heatmap analysis was used to assess simultaneous detections across the four replicates for each method and flask. The central trends in intensities between the different methods were compared by considering the median, which we chose to use because it is not affected by outliers or extreme values, making it a more robust measure of central tendency for datasets with skewed or heavy-tailed distributions. Venn diagrams were constructed to visualize the distribution of metabolites detected between the various culture flasks for each method. At another time, other statistical and mathematical tools were used to evaluate the extraction methodology's performances according to the four criteria noted previously: the number of features detected, their reproducibility (reproducible ion detection in replicates), the signal intensity, and the variability of the measured intensities.

UNDERSTANDING RESULTS

Untargeted metabolomics using HILIC- LC-HRMS allowed the detection of a metabolite set for each extraction method used. A total of 48 spectra were obtained, as explained previously and depicted in Figure 1, with four replicates (two technical replicates injected twice in the LC-HRMS system) per combination of flask and method. After processing and applying robustness filters, a total of 9122 unique features were retained across the three methods, meaning that 9122 features were observed at least once in any of the 48 spectra. These features were preliminarily visualized in a heatmap that can be found in the Supplemental Information (Fig. S1). In this heatmap, the clustering into three groups largely aligns with the extraction methods, with distinct zones of heat (red, signifying higher relative intensity). However, due to the number of samples and features, this plot is difficult to interpret, and we therefore visualized the data by different means.

A set of analytical criteria was used to judge the most complete extraction method for intracellular metabolites analyzed by HILIC chromatography: the number of metabolites recovered from *Tb. brucei*, their reproducibility, their intensity, and their specificity. In untargeted metabolomics, analysis quality depends strongly on the properties of the extraction workflow. The reproducibility and intensity of the relevant peaks are important criteria in selecting an appropriate extraction solvent. Based on the aforementioned criteria, M2 resulted in the most effective extraction method using the current analytical system and specifications. This is an important consideration—use of a HILIC column has been linked with better performance when studying hydrophilic metabolites, but it may reduce the detection of lipophilic compounds and thus change the overall picture of the trypanosome metabolome (Cubbon et al., 2010; Tang et al., 2016; Wang et al., 2019). To target the lipidome, this analysis can be redone using a different column (e.g., C18) or a column-switching system, if available. In that case, it is possible that the analytical outcomes and identifiable metabolites might change; hence, the choice of methodology should be adapted to the purpose of the study. Still, under the conditions described in this protocol for untargeted metabolomics using HILIC-LC-HRMS chromatography, the superior extraction method consisted of an acetonitrile/methanol/water mixture, as this led to the identification of a high number of parasitic metabolic pathways. A more detailed guide to the data we obtained and how to interpret it is provided below.

Principal component analysis for visualization of the spectra

Before any analysis was performed, a $\log(x+1)$ transformation was applied to the data to get a distribution of metabolomics data closer to normality, which allows the use of statistical models.

Published in : Current Protocols in Microbiology *(2024), vol. 4, 1043*
DOI: https://doi.org/10.1002/cpz1.1043
Status : Postprint (Author's version)

This choice also has a desirable property in regard to feature detection of ensuring that if the intensity of a feature was 0 before transformation, it remains 0 after tranformation.

Our PCA analysis is shown in Figure 2. It was first performed on the 48 spectra in order to highlight differences and similarities between the extraction methods and possible differences between flasks. The two first pricipal components explain 63.2% of the variability (PC1: 40.6% and PC2: 22.6%), which is not negligible. This 63.2% was observed from two stand points: per extraction method and per culture flask. On the scores plot that identifies samples per extraction method, they clearly seem to cluster according to method. On the other hand, on the scores plot where samples are identified by the flask they originate from, samples from the same flasks do not agglomerate together. This seems to indicate that the variability of the data explained by these two components, and that represents 63.2% of the data's variability, is correlated to the extraction method and not the flask. Hence, the methodology, not the biological inherent variability, is the most significant factor (>60%) in describing the metabolomic data.

This was further confirmed with an ASCA+ analysis. An ANOVA 2 model with two factors (method and flask) but without interaction was fitted to each response variable (*m/z*) and then subjected to a global measure and bootstrap test of factor importance. Table 2 shows the results and confirms that the extraction method is the greatest source of variability in the data and highly significant ($p < .001$). It is followed by the intragroup variability (shown as residuals) and finally by the flask. Although small, the flask effect is still very significant ($p < .001$).

ASCA-E provides also a decomposition of the original PCA score plot into score plots linked to each source of variability. Figure 3 shows, as expected, a major difference between extraction methods (Fig. 3A) and that the significant difference between flasks is mainly due to a difference between flasks 1 and 2 and flasks 3 and 4 (Fig. 3B). The residuals score plot (Fig. 3C) shows that the biggest intra-group variability is observed for method 3, followed here by method 2 and then method 1. This last graph must nevertheless be interpreted with caution because only 29% of the residual variability is explained by PC1 and PC2. It is important to note that although M1 and M3 involve mixtures of the same extraction solvents, the ratios of the mixture are not the same, and this, along with the fact that samples underwent a simple incubation in M1, whereas M3 involves sonication plus agitation during sampling, may be related to the intra- group variability displayed.

Figure 2 *Principal component analysis (PCA) score plots of metabolic profiles of Tb. brucei with the three different extraction methods (M1, M2, and M3; left) using four different cultures (F1, F2, F3, and F4; right)*

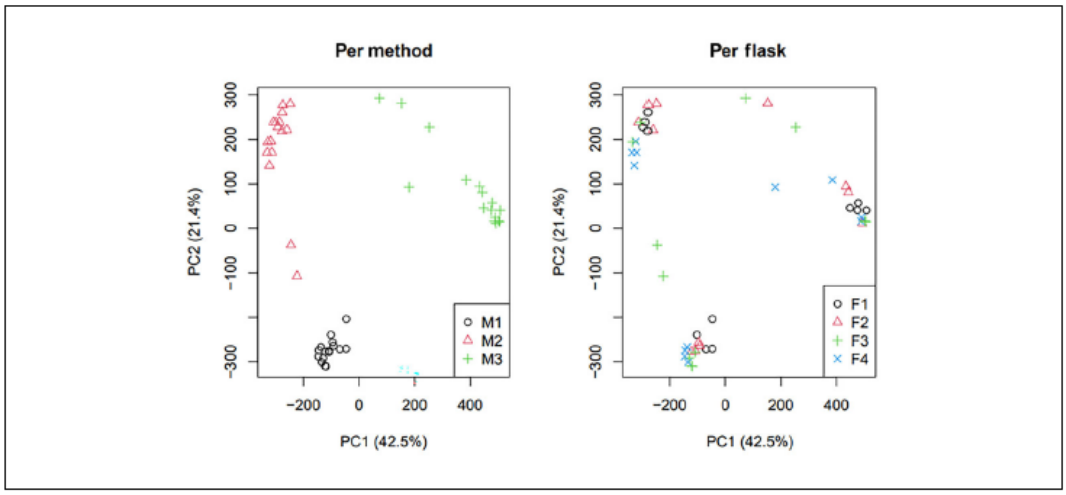

Table 2 *Quantification of the Sources of Variability in the Data with ASCA Percentage of Variance and Statistical Significance*

	Method	Flask	Residuals
% of variance explained[a]	55.14 %	5.74%	39.12%
Boostrap *p*-value	$p < .001$	$p < .001$	–

[a]The extraction method is the greatest source of variability in the data, with a highly significant effect ($p < .001$). That is followed by the intragroup variability and finally flask-related variability. Although low, the flask effect is highly significant ($p < .001$).

Figure 3 *ASCA-E score plots and residuals for model effects due to methods and flasks. As expected, there is a substantial difference between extraction methods (**A**); the significant difference between flasks is due mainly to a difference between flasks F1 and F2 versus F3 and F4 (**B**). The residuals score plot (**C**) shows that the greatest intra-group variability is observed for method M3, followed by M2 and then M1. This last graph must nevertheless be interpreted with some caution because only 29% of the residual variability is explained by PC1 and PC2.*

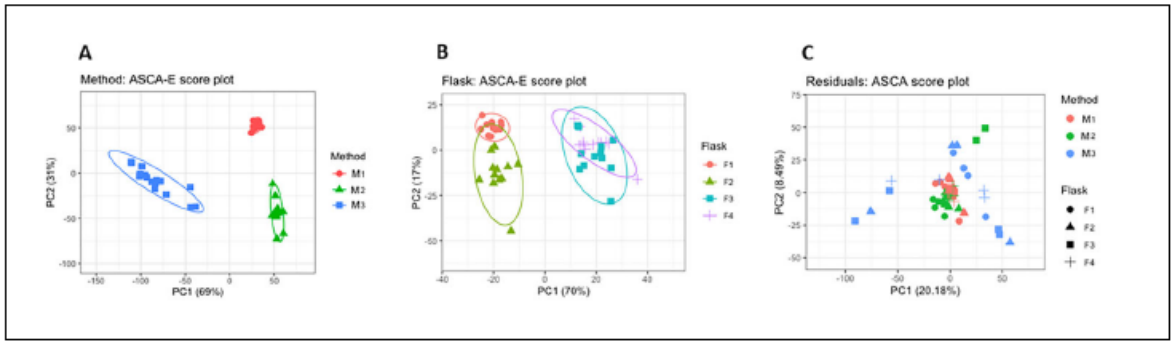

Published in : Current Protocols in Microbiology *(2024), vol. 4, 1043*
DOI: https://doi.org/10.1002/cpz1.1043
Status : Postprint (Author's version)

Table 3 *Number of Features Detected*

	Average count F1	Average count F2	Average count F3	Average count F4	Average (SD) count F1-F4	Total count (different features)
M1	6405.50	6311.25	6306.50	6521.25	6386.13 (333.38)	7901
M2	7009.75	6938.75	7142.50	7342.00	7108.25 (275.37)	8471
M3	5199.25	5375.25	5552.0	5686.25	5453.19 (850.25)	8155
M1-M3						9122

Each cell represents the average over four replicates of the count of features detected per method and flask combination. The rightmost two columns show the average across flasks per method (with standard deviation, SD) and the total number of different features detected at least once with a given method in at least one spectrum. Different sets of features might be detected in different replicates; therefore, their total number is also reported at least once per method (9122 features aggregating across methods). M2 displays a higher average detected features across flasks and total different features.

Number of features detected by each method

Table 3 shows the sensitivity of detection in the sense of the number of features that give a nonzero intensity in a spectrum. The average count across the four replicates is presented for a given combination of method and flask. The results in Table 3 indicate that M2, in which the extraction solvent is 4:4:2 (v/v/v) acetonitrile/methanol/water, allows the detection of the largest number of features. An average of 7108 features per spectrum were detected with M2, followed by 6386 features for M1 and 5453 features for M3.

Intensity and variability of measured signals

The intensity and variability of the measured signal are important factors to evaluate if a method is consistent. An extraction method should reveal the most complete metabolome possible, which translates into the number of features, but these need to be reliably detected each time, as otherwise their variability will be too high for them to be adequately used for biological interpretation. As such, in order to better characterize the methods, several summary statistics are computed describing the intensity of the ions. First, 16 measurements (four flasks and four replicates) associated with each feature are summarized to obtain three main characteristics—mean, standard deviation, and coefficient of variation (obtained by dividing the latter by the

former)— for each feature and method. This summary is presented in Table 4 and visualized as classic boxplots in Figure 4. A filter for each series is introduced, retaining only features detected in at least one of the four flasks for a given method and with a signal in at least three of the four replicates. Results show that M2 is superior to the other methods tested because of the higher mean and lower variability of the signal. M3 is the weakest of them in terms of signal intensity and variability. Variations during the experimental process for any extraction method can account for variations in the intensity of the detected signals. Changes to incubation times with the mixture of extraction solvent, variations to temperature in case of sonication, or the necessity to evaporate the solvent prior to resuspension and analysis can all be contributing factors.

Reproducibility across flasks and methods

The experiment was also designed to determine the reproducibility across replicates: namely, the extent to which the same feature was detected in the different replicates. Initially, the reproducibility across the four replicates in a given combination of flask and method was analyzed. Subsequently, reproducibility across flasks in a given method was determined. Reproducibility was analyzed as the variability of the intensity of the measured signal across replicates for a given feature.

Table 4 *Mean (Median) Across the Series of 16 Measurement Summaries, Retaining Only Features Detected in at Least One Flask (Counts Shown in Column Headers)*

	M1 (7,035)	M2 (7,688)	M3 (5,967)
Mean (median) over feature means	11.21 (11.90)	11.76 (12.26)	10.32 (10.66)
Mean (median) over feature SDs	2.21 (0.98)	2.14 (0.91)	3.16 (3.28)
Mean (median) over feature CVs	0.30 (0.077)	0.26 (0.071)	0.41 (0.29)

Columns represent the methods (with counts shown in parentheses); rows define the type of summary per feature: means (row 1), standard deviations (SD; row 2), and coefficients of variation (CV, the ratio SD/mean; row 3), respectively. M2 has, for a total of more detected features in at least one flask (7688), a slightly higher mean of feature means and a lower SD and CV.

Figure 4 *Intensity levels and measurement variability for the three methods. Classic boxplots represent the interquartile range of 9122 values, one per ion. The whiskers represent the limits to define outliers calculated by subtracting 1.5× the interquartile range from the 25th percentile, or adding to the 75th percentile. The horizontal lines denote the mean over 16 replicates, the standard deviation over 16 replicates and the*

Published in : Current Protocols in Microbiology *(2024), vol. 4, 1043*
DOI: https://doi.org/10.1002/cpz1.1043
Status : Postprint (Author's version)

associated coefficient of variation, respectively. M1 and M2 seem fairly similar in regard to the mean intensity and variability of intensity per ion, but M2 shows the smallest coefficient of variability.

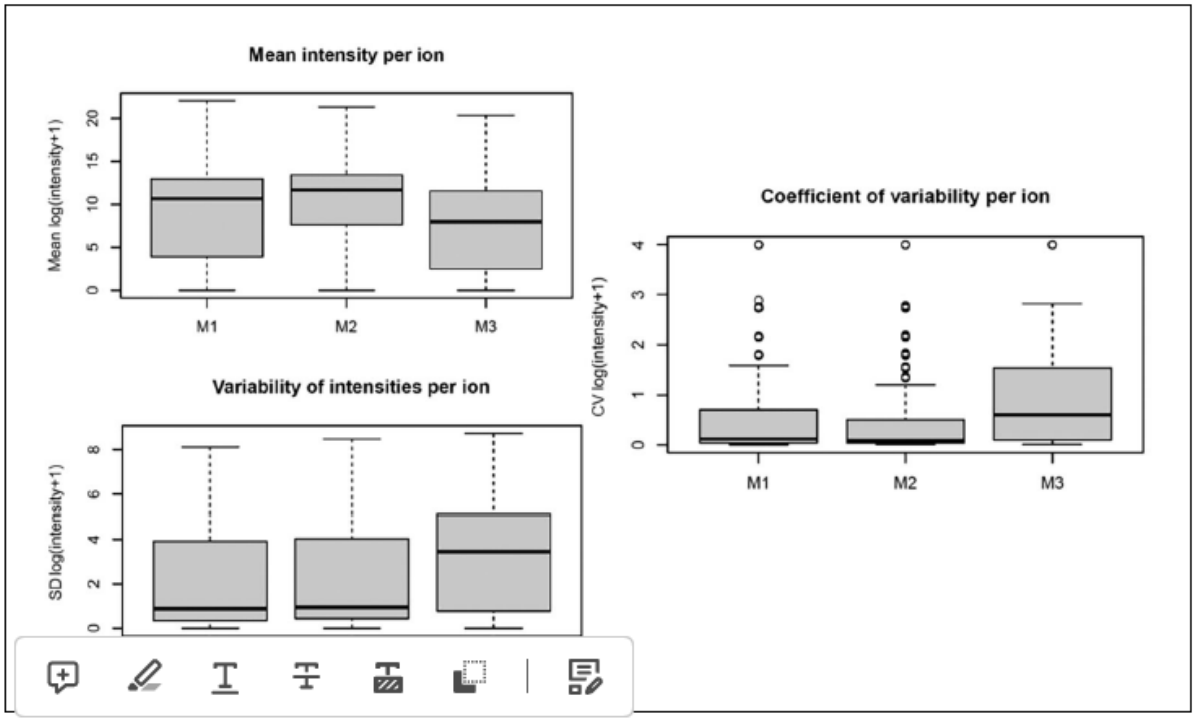

Table 5 Percentage of Features as a Function of the Level of Detection Across Replicates

	0	1	2	3	4	**3-4**
Method 1	20.7%	5.5%	5.8%	9.0%	59.0%	**68.0%**
Method 2	13,7%	4.4%	5.8%	8.7%	67.4%	**76.1%**
Method 3	22.0%	11.9%	12.1%	12.9%	41.1%	**54.0%**

Columns represent the replicates, i.e., the first column indicates the percentage of features not detected in any replicate, the second column those only detected in one replicate, and so on. The second-to-last column represents features detected in at least three out of four replicates as useful but according to less strict criteria, to summarize findings across the four replicates. M2 accounted for the smallest number of features detected in none of the replicates (13.7%) and the largest number of features detected in three or four replicates or in all four replicates. The total (100%) corresponds to 9122.

Table 5 shows the percentage of the features as a function of the level of detection across replicates. The majority of features are detected in a reproducible way across the replicates: that is, most features (>50%, 60%, or 70%) are detected in at least three out of four replicates. Method 2 allows the largest number of features to be detected, followed by Method 1 and then Method 3.

Simultaneous identifications across the four replicates for each method (M1-M3) and flask (F1-F4) combination are visualized using a heatmap, as shown in Figure 5. The first column, corresponding to the percentage of features found in none of the four replicates, and the last column, corresponding to features detected in all four replicates, show the darkest colors; hence, the highest percentage of features detected were in either none or all of the replicates. This visualization also makes it possible to infer directly that the higher percentage of detected features was achieved with M2, followed by M1 and M3.

Figure 5 *Heatmap analysis to assess simultaneous detections across the four replicates (reps) for each method (M1-M3) and flask (F1-F4) combination (rows). Columns correspond to how many simultaneous detections are seen (from 0 to 4 out of 4), and the cell color intensity increases with the percentage of features (from a total of 9122) that have that level of detection.*

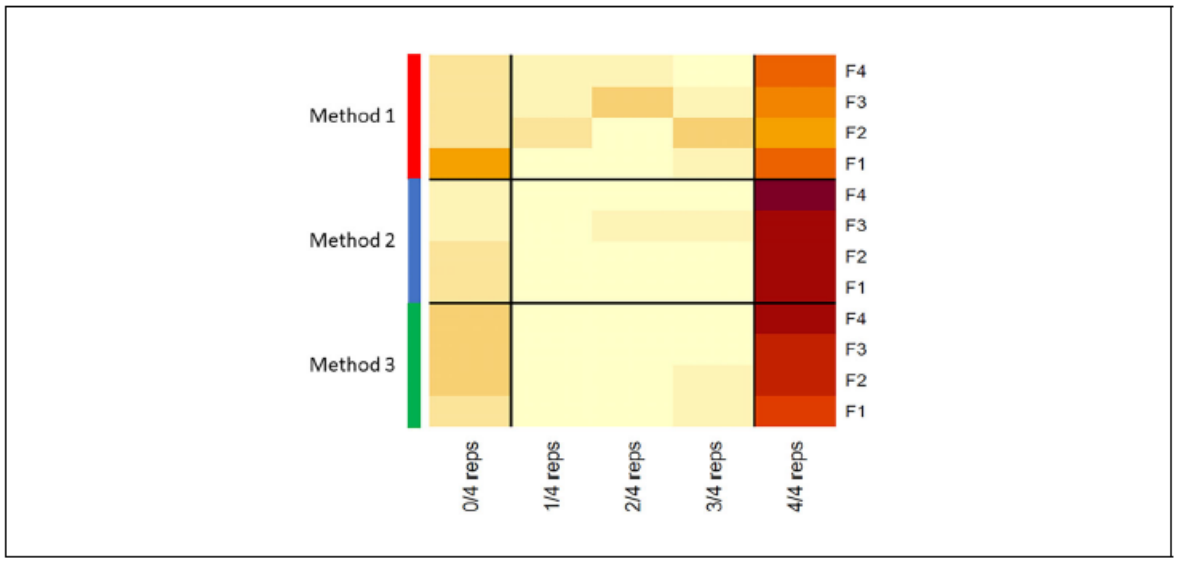

Figure 6 *Venn diagrams representing the breakdown of the total 9122 features over the flasks. One diagram is shown per method, with panels* ***A****,* ***B****, and* ***C*** *representing methods M1, M2, and M3, respectively. A feature is counted in an intersection when it is detected in all corresponding sets; any feature not detected in any flask is counted in the percentage undetected (represented outside the diagram). M2 has the lowest percentage of undetected features (15.7%) and the highest percentage of features that were detected consistently across the four flasks (65.1%).*

Published in : Current Protocols in Microbiology *(2024), vol. 4, 1043*
DOI: https://doi.org/10.1002/cpz1.1043
Status : Postprint (Author's version)

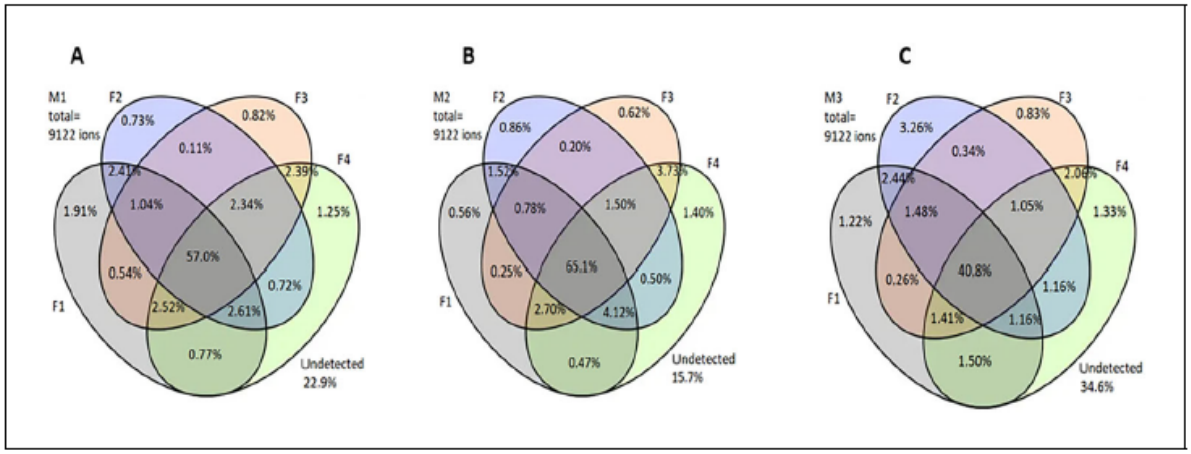

To determine the reproducibility across flasks, the notion of the detection of a feature with each method and flask has first to be defined. Here, a feature is considered detected with a method for a specific flask when it is observed in at least three out of four replicates. Therefore, to evaluate reproducibility, a set of Venn diagrams displaying the features detected per flask as extracted for M1, M2, or M3 are shown in Figure 6.

Here, each diagram relates to an extraction method (M1, M2, or M3), and the total number of features (100% = 9122 peaks) is broken down over the sets (or flasks) according to where the features are detected. Many features are detected simultaneously in all four flasks (intersection of the four sets), some are detected in only a few flasks, while some substantial percentage are not detected in any flask (represented outside of the Venn diagram). M2 has the lowest percentage of un- detected features (15.7%) and the highest percentage of features that are detected consistently across the four flasks (65.1%), and is thus the most reproducible.

Figure 7 *Differentiation of detected ions per flask and method. Each Venn diagram represents a flask, with the totality of features that are detected simultaneously with the three methods, detected with two methods, specific to a method, or not detected (in red, outside the diagram) indicated. The number of features associated with the three extraction methods per flask stays relatively similar, but there are variations related to specific method features. For all flasks, M2 accounts for the most uniquely specific features, followed by M3 and M1.*

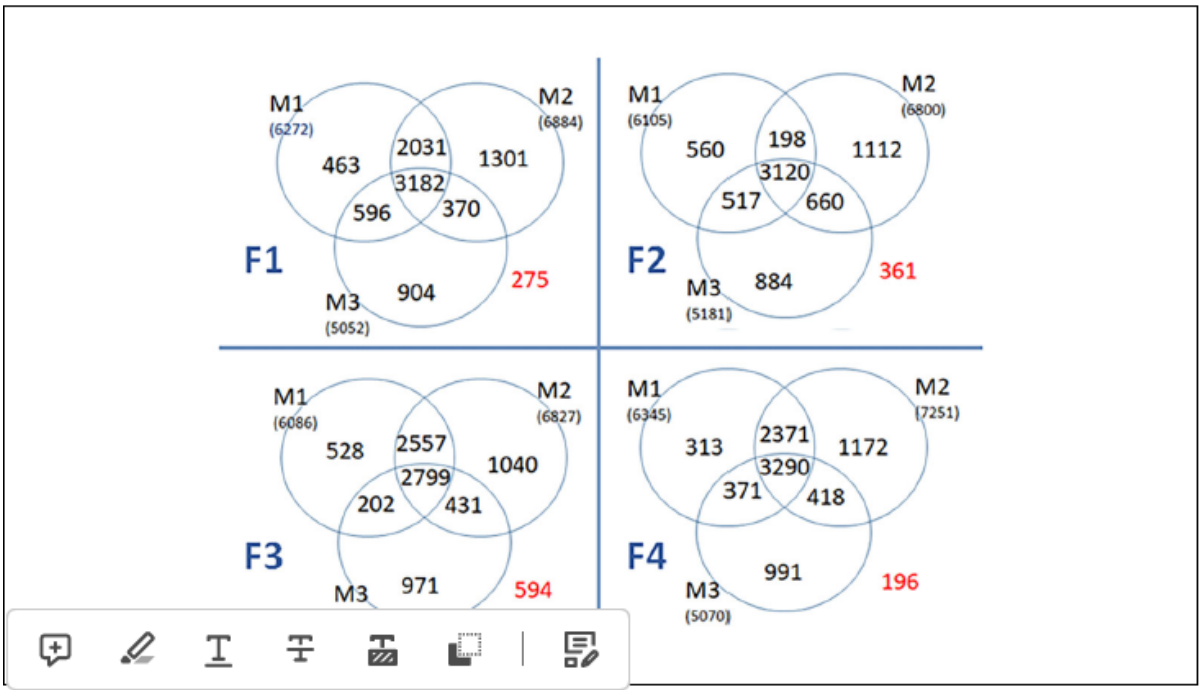

Identification of method-specific ions/annotations

The final step to evaluate whether an extraction method succeeds in covering the metabolome robustly relates to feature identification. As mentioned previously, in untargeted metabolomics, the objective is to gather an extensive overview of metabolism, insofar as possible. Before annotation was attempted, a last visualization explored whether ions were detected similarly across all methods of extraction. The number of features detected with the methods are reported in a Venn diagram per flask in Figure 7. In each diagram, three sets represent the methods and allow the counting of however many features are simultaneously detected across two or three methods or are specific to a single method. The number of features associated with the three extraction methods per flask stays relatively similar, but variations are found related to feature of the specific methods. For all flasks, M2 accounts for more uniquely specific features, followed by M3 and M1.

In metabolomics, annotation of metabolites is essential to give biological meaning to the data and to understand underlying biological mechanisms, which can have a multitude of applications (Fall et al., 2022). Initially, all features found across all extraction methods were explored and annotated with a Mummichog algorithm and visualized in a scatter plot (Figure 8A). This annotation is performed with the Metaboanalyst module that uses the KEGG database associated with *Tb. brucei* based on the *m/z* ratio and immediately indicates visually whether a pathway is extensively present or not (Chong et al., 2018). In this initial analysis, metabolites associated with 54 distinct trypanosome metabolic pathways were found, and of these, 14 pathways had all of their metabolites

Published in : Current Protocols in Microbiology *(2024), vol. 4, 1043*
DOI: https://doi.org/10.1002/cpz1.1043
Status : Postprint (Author's version)

identified. This represents an extensive annotation and indicates that a broad variety of metabolites were extracted and detected across methodologies. Notably, obtaining a major overview of pathways related to amino acid metabolism, cofactor and vitamin metabolism, carbohydrate metabolism, and lipid metabolism is indicative of robust detection across samples.

In addition, we were interested in investigating which extraction method gave the most varied overview of the metabolome, and whether these methods were focused on specific pathways. To achieve this, the databases were separated based on the exclusivity of the features detected. That is, for each extraction method, a feature had to be found in three or four replicates of this method, but found in less than two replicates for any other method. Results are shown for each method in Figure 8B-D in the form of the KEGG metabolic pathway network associated with *Tb. brucei.* Visually, it is evident that M1 presents fewer metabolites than M2 and M3, and it also illustrates fewer pathways, meaning less variety in the types of metabolites detected. The workflow of the extraction methods can be directly correlated to the type, variety, and number of metabolites detected. A distinction can be observed in regard to carbohydrate metabolism, in which for M1 fewer metabolites and pathways were found. Specifically, the TCA cycle and pyruvate metabolism are among the pathways more often detected with M2 and M3, rather than M1. Moreover, there is another difference in regard to the metabolism of amino acid and related com- pounds, for which M1 also has fewer hits than M2 and M3. M1 includes 1 h of agitation to extract metabolites, whereas both M2 and M3 involve extractions of only 20 min. This distinction might be related to metabolite turnover and justify the profile distinction.

Figure 8 *Graphical visualization of the pathways detected and ions annotated. (**A**) Pathway analysis plot using Mummichog, with matched pathways displayed as circles. The color and size correspond to the enrichment factor—that is, the ratio between number of the hits found and the number of expected compounds within a pathway. The p-value correlates to the ANOVA automatically generated between extraction methods and, as such, the most differentially detected pathway between the methods is that of arginine and proline metabolism. (**B, C, and D**) Tb. brucei global metabolic networks generated through KEGG for M1 (**B**), M2 (**C**), and M3 (**D**). Colored circles represent hits detected through the Mummichog pathway analysis and their colors represent the type of metabolism being affected: red for nucleotide metabolism, green for metabolism of amino acids and related compounds, yellow for carbohydrate metabolism, orange for lipid metabolism, and blue for cofactor and vitamin metabolism.*

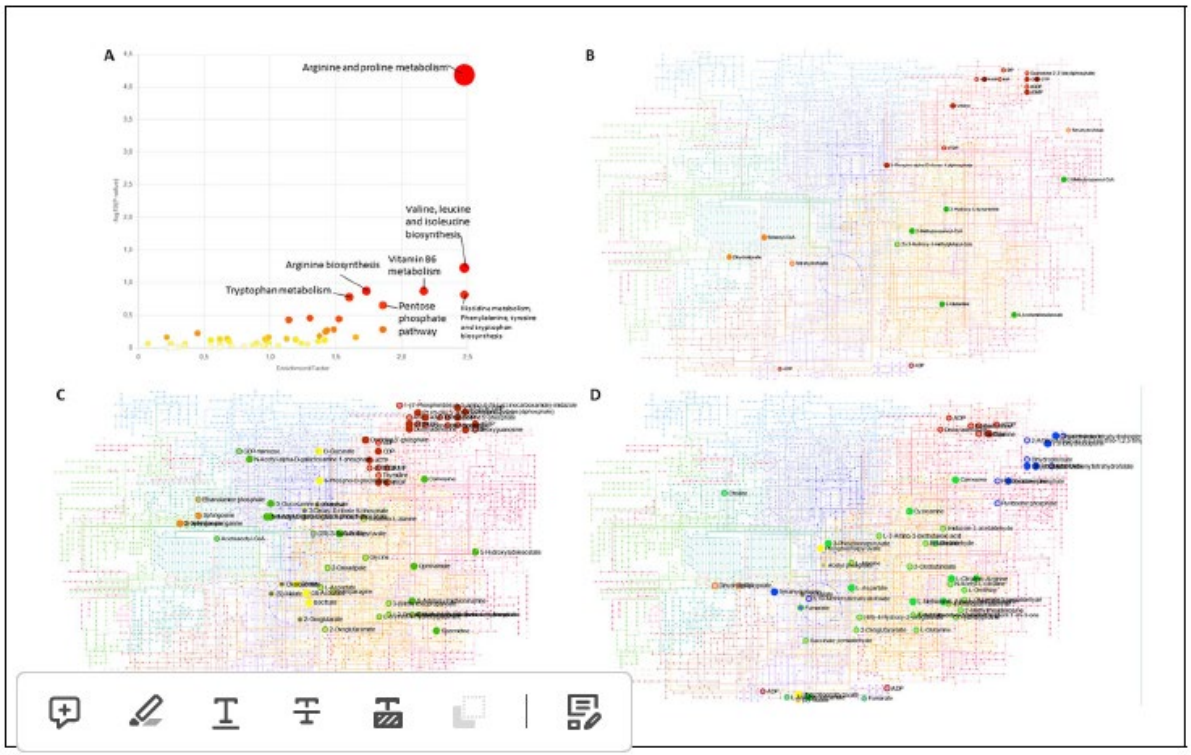

Additionally, even though the same solvents are used for extraction in M1 and M3, the mixtures (ratios) of those solvents are dissimilar: the mixture for M1 is mostly hydrophilic, whereas that for M3 is the opposite. How-ever, the apolar phase of the M3 extract is not analyzed, and thus information is lost in this stage. This might explain why M3 samples do not report more lipidic metabolites than other methods, since the Bligh and Dyer method is used preferentially to extract lipid metabolites (Breil et al., 2017). As such, it would be interesting to use a reverse-phase (RP) chromatography column to analyze the nonpolar molecules.

Interestingly, M1 shows fewer exclusive features (265) than M3 (804 features), which might be related to both the hydrophilic nature of the extract solvent mixture for M1 and the long experimental time. Notably, M3 distinctly shows metabolites that are part of cofactor and vitamin metabolism, which might represent an advantage if that pathway is of interest in a given study. Lastly, M2 shows a larger list of exclusive features (970), which correlated to a higher number of hits and pathways being detected. This, along with the robustness of the method according to the parameters evaluated above, leads us to conclude that for the analytical method proposed (HILIC HPLC-HRMS), M2 yields the most complete untargeted profile, which could be useful for other trypanosome metabolomic tests. Nevertheless, the information gathered by all three methods combined was more extensive than that provided by any one method alone, which is in line with the truism that no single extraction method can achieve a complete set of metabolites.

Published in : Current Protocols in Microbiology *(2024), vol. 4, 1043*
DOI: https://doi.org/10.1002/cpz1.1043
Status : Postprint (Author's version)

Time Considerations

Basic Protocol 1: Thawing and re-culturing of trypanosomes takes ~2 weeks. For the metabolomic analysis, the four flasks were cultured for 3 days.

Basic Protocol 2: Extractions take 2 days.

Basic Protocol 3: Mass spectrometry analysis lasted 2.5 days. Data processing takes be- tween 1 and 4 weeks depending on the availability of researchers and data analysts.

Acknowledgments

Fanta Fall has a post-doctoral grant and Lucia Mamede a doctoral grant as part of the METNATPAR PDR project (T.0092.20) funded by FNRS. LC-MS analysis was performed at the MASSMET platform.

Author Contributions

Fanta Fall: Conceptualization; data curation; methodology; validation; visualization; writing—original draft. **Lieven Desmet**: Conceptualization; data curation; methodology; writing—original draft; writing—review and editing. **Laura Schioppa**: Writing—original draft; writing—review and editing. **Lucia Mamede**: Writing—original draft; writing— review and editing. **Pascal De Tullio**: Conceptualization; supervision; writing—review and editing. **Michel Frédérich**: Conceptualization; supervision; writing—review and editing. **Bernadette Govaerts**: Conceptualization; methodology; supervision; writing—review and editing. **Joëlle Quetin- Leclercq**: Conceptualization; methodology; supervision; writing—review and editing.

Conflict of Interest

The authors declare no conflict of interest.

Data Availability Statement

The data supporting the findings of this study are available at *https:// forge.uclouvain. be/ smcs/metnatpar.git*

Supporting Information

cpz11043-sup-0001-SuppMat.docx

Supplemental Figure S1 Heatmap with hierarchical clustering (complete linkage, euclidean

distance) showing intensities of the 9222 features across all 48 samples. The clustering tends to reproduce the grouping of samples by extraction method.

Bibliography

Adusumilli, R., & Mallick, P. (2017). Data conversion with ProteoWizard msConvert. *Methods in Molecular Biology*, *1550*, 339-368. https://doi. org/10.1007/978- 1-4939-6747-6_23

Amiar, S., Katris, N. J., Berry, L., Dass, S., Duley, S., Arnold, C. S., Shears, M. J., Brunet, C., Touquet, B., McFadden, G. I., Yamaryo-Botté, Y., & Botté, C. Y. (2020). Division and adaptation to host environment of apicomplexan parasites depend on apicoplast lipid metabolic plasticity and host organelle remodeling. *Cell Reports*, *30*(11), 3778-3792. e9. https://doi.org/ 10.1016/j.celrep.2020.02.072

Bakker, B. M., Michels, P. A. M., Opperdoes, F. R., & Westerhoff, H. V. (1999). What controls glycolysis in bloodstream form *Trypanosoma brucei*? *Journal of Biological Chemistry*, *274*(21), 14551-14559. https://doi.org/10.1074/jbc.274. 21.14551

Bi, H., Krausz, K. W., Manna, S. K., Li, F., Johnson, C. H., & Gonzalez, F. J. (2013). Optimization of harvesting, extraction, and analytical protocols for UPLC-ESI-MS- based metabolomic analysis of adherent mammalian cancer cells. *Analytical and Bioanalytical Chemistry*, *405*(15), 5279-5289. https://doi.org/10.1007/s00216-013-6927-9

Breil, C., Abert Vian, M., Zemb, T., Kunz, W., & Chemat, F. (2017). “Bligh and Dyer” and Folch Methods for solid-liquid-liquid extraction of lipids from microorganisms. Comprehension of solvatation mechanisms and towards substitution with alternative solvents. *International Journal of Molecular Sciences*, *18*(4), 708. https://doi.org/10.3390/ijms18040708

Brun, R., Blum, J., Chappuis, F., & Burri, C. (2010). Human African trypanosomiasis. *The Lancet*, *375*(9709), 148-159. https://doi.org/10. 1016/S0140-6736(09)60829-1

Chong, J., Soufan, O., Li, C., Caraus, I., Li, S., Bourque, G., Wishart, D. S., & Xia, J. (2018). MetaboAnalyst 4.0: Towards more transparent and integrative metabolomics analysis. *Nucleic Acids Research*, *46*(W1), W486-W494. https: //doi.org/10.1093/nar/gky310

Creek, D. J., Mazet, M., Achcar, F., Anderson, J., Kim, D. H., Kamour, R., Morand, P., Millerioux, Y., Biran, M., Kerkhoven, E. J., Chokkathukalam, A., Weidt, S. K., Burgess, K. E., Breitling, R., Watson, D. G., Bringaud, F., & Barrett, M. P. (2015). Probing the metabolic network in bloodstream-form *Trypanosoma brucei* using untargeted metabolomics with stable isotope labelled glucose. *PLoS Pathogens*, *11*(3), e1004689. https://doi.org/10.1371/journal.ppat. 1004689

Cubbon, S., Antonio, C., Wilson, J., & Thomas- Oates, J. (2010). Metabolomic applications of HILIC-LC-MS. *Mass Spectrometry Reviews*, *29*(5), 671-684. https://doi.org/10.1002/ mas.20252

Fall, F., Mamede, L., Schioppa, L., Ledoux, A., de Tullio, P., Michels, P., Frédérich, M., & Quetin-Leclercq, J. (2022). *Trypanosoma brucei*: Metabolomics for analysis of cellular metabolism and drug discovery. *Metabolomics*, *18*(4), 20. https://doi.org/10.1007/s11306-022- 01880-0

Giacomoni, F., le Corguillé, G., Monsoor, M., Landi, M., Pericard, P., Pétéra, M., Duperier, C., Tremblay-Franco, M., Martin, J. F., Jacob, D., Goulitquer, S., Thévenot, E. A., & Caron, C. (2015). Workflow4Metabolomics: A collaborative research infrastructure for computational metabolomics. *Bioinformatics*, *31* (9), 1493-1495. https://doi.org/ 10.1093/bioinformatics/btu813

Hannaert, V. (2011). Sleeping sickness pathogen (*Trypanosoma brucei*) and natural products: Therapeutic targets and screening systems. *Planta Medica*, *77*(6), 586-597. https://doi.org/ 10.1055/s-0030- 1250411

Hirumi, H., & Hirumi, K. (1994). Axenic culture of African trypanosome bloodstream forms. *Parasitology Today*, *10*(2), 80-84. https://doi.org/10. 1016/0169-4758(94)90402-2

Johnson, C. H., Ivanisevic, J., & Siuzdak, G. (2016). Metabolomics: Beyond biomarkers and towards mechanisms. *Nature Reviews. Molecular Cell Biology*, *17*(7), 451-459. https://doi. org/10.1038/nrm.2016.25

Johnston, K., Kim, D.-H., Kerkhoven, E. J., Burchmore, R., Barrett, M. P., & Achcar, F. (2019). Mapping the metabolism of five amino acids in bloodstream form *Trypanosoma brucei* using U-^{13}C-labelled substrates and LC- MS. *Bioscience Reports*, *39*(5), BSR20181601. https://doi.org/10.1042/BSR20181601

Kafsack, B. F. C., &Llinâs, M. (2010). Eating at the table of another: Metabolomics of host/parasite interactions. *Cell Host & Microbe*, *7*(2), 90-99. https://doi.org/10.1016/j.chom.2010.01.008

Kamleh, A., Barrett, M. P., Wildridge, D., Burchmore, R. J. S., Scheltema, R. A., & Watson, D. G. (2008). Metabolomic profiling using Orbitrap Fourier transform mass spectrometry with hydrophilic interaction chromatography: A method with wide applicability to analysis of biomolecules. *Rapid Communications in Mass Spectrometry: RCM*, *22*(12), 1912-1918. https://doi.org/10.1002/rcm.3564

Kanehisa, M., & Goto, S. (2000). KEGG: Kyoto Encyclopedia of Genes and Genomes. *Nucleic Acids Research*, *28*(1), 27-30.

Madji Hounoum, B., Blasco, H., Emond, P., & Mavel, S. (2016). Liquid chromatography- high-resolution mass spectrometry-based cell metabolomics: Experimental design, recommendations, and applications. *TrAC Trends in Analytical Chemistry*, *75*, 118-128. https://doi. org/10.1016/j.trac.2015.08.003

Mamede, L., Fall, F., Schoumacher, M., Ledoux, A., de Tullio, P., Quetin-Leclercq, J., & Frédérich, M. (2022). Recent metabolomic developments for antimalarial drug discovery. *Parasitology Research*, *121*(12), 3351-3380. https://doi.org/10.1007/s00436-022-07673-7

Martin, A. C., Pawlus, A. D., Jewett, E. M., Wyse, D. L., Angerhofer, C. K., & Hegeman, A. D. (2014). Evaluating solvent extraction systems using metabolomics approaches. *RSC Advances*, *4*(50), 26325-26334. https://doi.org/10. 1039/C4RA02731K

Matthews, K. R. (2005). The developmental cell biology of *Trypanosoma brucei*. *Journal of Cell Science*, *118*(2), 283-290. https://doi.org/ 10.1242/jcs.01649

Pineda, E., Thonnus, M., Mazet, M., Mourier, A., Cahoreau, E., Kulyk, H., Dupuy, J. W., Biran, M., Masante, C., Allmann, S., Rivière, L., Rotureau, B., Portais, J. C., & Bringaud, F. (2018). Glycerol supports growth of the *Trypanosoma brucei* bloodstream forms in the absence of glucose: Analysis of metabolic adaptations on

glycerol-rich conditions. *PLOS Pathogens*, *14*(11), e1007412. https://doi.org/ 10.1371/journal.ppat.1007412

Pinu, F. R., Villas-Boas, S. G., & Aggio, R. (2017). Analysis of intracellular metabolites from microorganisms: Quenching and extraction proto- cols. *Metabolites*, *7*(4), 53. https://doi.org/10. 3390/metabo7040053

R: The R Project for Statistical Computing. (n.d.). https://www.r-project.org/

Rey-Stolle, F., Dudzik, D., Gonzalez-Riano, C., Fernândez-Garrfa, M., Alonso-Herranz, V., Rojo, D., Barbas, C., & Garrfa, A. (2022). Low and high resolution gas chromatography-mass spectrometry for untargeted metabolomics: A tutorial. *Analytica Chimica Acta*, *1210*, 339043. https://doi.org/10.1016/j.aca.2021.339043

Richmond, G. S., Gibellini, F., Young, S. A., Major, L., Denton, H., Lilley, A., & Smith, T. K. (2010). Lipidomic analysis of bloodstream and procyclic form *Trypanosoma brucei*. *Para- sitology*, *137*(9), 1357-1392. https://doi.org/10. 1017/S0031182010000715

Smith, C. A., Want, E. J., O'Maille, G., Abagyan, R., & Siuzdak, G. (2006). XCMS: Processing mass spectrometry data for metabolite profiling using nonlinear peak alignment, matching, and identification. *Analytical Chemistry*, *78*(3), 779-787. https://doi.org/10.1021/ac051437y

Smith, T. K., Bringaud, F., Nolan, D. P., & Figueiredo, L. M. (2017). Metabolic reprogramming during the *Trypanosoma brucei* life cycle. *F1000Research*, *6*, 683. https://doi.org/10. 12688/f1000research.10342.2

Song, X., Yang, X., Ying, Z., Wu, K., Liu, J., & Liu, Q. (2023). Regulation of mitochondrial energy metabolism by glutaredoxin 5 in the api-complexan parasite *Neospora caninum*. *Microbiology Spectrum*, *11*(1), e0309122. https://doi. org/10.1128/spectrum.03091-22

t'Kindt, R., Jankevics, A., Scheltema, R. A., Zheng, L., Watson, D. G., Dujardin, J. C., Breitling, R., Coombs, G. H., & Decuypere, S. (2010). Towards an unbiased metabolic pro- filing of protozoan parasites: Optimisation of a Leishmania sampling protocol for HILIC-Orbitrap analysis. *Analytical and Bioanalytical Chemistry*, *398*(5), 2059-2069. https://doi.org/ 10.1007/s00216-010-4139-0

Tang, D.-Q., Zou, L., Yin, X.-X., & Ong, C. N. (2016). HILIC-MS for metabolomics: An attractive and complementary approach to RPLC-MS. *Mass Spectrometry Reviews*, *35*(5), 574-600. https://doi.org/10.1002/mas.21445

Thiel, M., Benaiche, N., Martin, M., Franceschini, S., van Oirbeek, R., & Govaerts, B. (2023). limpca: An R package for the linear modeling of high-dimensional designed data based on ASCA/APCA family of methods. *Journal of Chemometrics*, *37*(7), e3482. https://doi.org/10. 1002/cem.3482

Thiel, M., Féraud, B., & Govaerts, B. (2017). ASCA+ and APCA+: Extensions of ASCA and APCA in the analysis of unbalanced multifactorial designs: Analyzing unbalanced multifactorial designs with ASCA+ and APCA+. *Journal of Chemometrics*, *31*(6), e2895. https://doi.org/ 10.1002/cem.2895

Vertommen, D., van Roy, J., Szikora, J.-P., Rider, M. H., Michels, P. A. M., & Opperdoes, F. R. (2008). Differential expression of glycosomal and mitochondrial proteins in the two major life-cycle stages of *Trypanosoma brucei*. *Molecular and Biochemical Parasitology*, *158*(2), 189201. https://doi.org/10.1016/j.molbiopara.2007. 12.008

Villafraz, O., Biran, M., Pineda, E., Plazolles, N., Cahoreau, E., Ornitz Oliveira Souza, R., Thonnus, M., Allmann, S., Tetaud, E., Rivière, L., Silber, A. M., Barrett, M. P., Zikovâ, A., Boshart, M., Portais, J. C., & Bringaud,

F. (2021). Procyclic trypanosomes recycle glucose catabolites and TCA cycle intermediates to stimulate growth in the presence of physiological amounts of proline. *PLOS Pathogens*, *17*(3), e1009204. https://doi.org/10.1371/journal.ppat. 1009204

Vincent, I. M., & Barrett, M. P. (2015). Metabolomic-based strategies for antiparasite drug discovery. *Journal of Biomolecular Screening*, *20*(1), 44-55. https://doi. org/10.1177/1087057114551519

Wang, S., Blair, I. A., & Mesaros, C. (2019). An- alytical methods for mass spectrometry-based metabolomics studies. *Advances in Experimental Medicine and Biology*, *1140*, 635-647. https: //doi.org/10.1007/978-3-030-15950-4_38

World Health Organization. (n.d.). *Human African trypanosomiasis (sleeping sickness)*. World Health Organization. http: //www.who.int/trypanosomiasis_african/en/

Zoltner, M., Campagnaro, G. D., Taleva, G., Burrell, A., Cerone, M., Leung, K. F., Achcar, F., Horn, D., Vaughan, S., Gadelha, C., Zikovâ, A., Barrett, M. P., de Koning, H. P., & Field, M. C. (2020). Suramin exposure alters cellular metabolism and mitochondrial energy production in African trypanosomes. *Journal of Biological Chemistry*, *295*(24), 8331-8347. https: //doi.org/10.1074/jbc.RA120.012355